# Design of a Machine Learning Model to Enhance the Arming of the System Integrity Protection Scheme of the Brazilian North-Southeast HVDC Bipoles

L. Zanella, B.A.S. Ambrósio, G.R. Moraes, I.C. Decker, A.F.C. Aquino, D. Issicaba
Federal University of Santa Catarina, Florianópolis–SC, Brazil
INESC P&D Brasil, Santos–SP, Brazil

***Abstract*—This paper presents the modeling and implementation of a customized Machine Learning (ML) model designed to take advantage of synchrophasor data to enhance the arming procedure of a critical System Integrity Protection Scheme (SIPS) of the Brazilian Interconnected Power System (BIPS). This model allows risk-averse decision-making, mitigating loss of selectivity conditions. Implementation has been achieved using applications developed in the Open and Extensible Control and Analytics (openECA) software environment. Results are obtained using simulations on a Real-Time Digital Simulator (RTDS) set-up, which has been provided with control and protection replicas of the high voltage direct current (HVDC) systems of the BIPS.**

***Index Terms*—WAMPAC, Machine Learning, RTDS, SIPS, HVDC.**

## I. Introduction

Over the years, power system operation has become progressively more complex, due to the demand increase, the integration of intermittent renewable generation, and the widespread application of inverter-based resources at the transmission and distribution levels. Consequently, power systems are currently subjected to more stressed and fast-changing operating conditions, with large variations in power interchanges among areas, where system-wide protection solutions are of utmost importance to prevent disturbance propagation. In this context, SIPSs [1] are needed to enhance security and prevent the degradation of power system performance in cases of nonsecure conditions or extreme contingencies.

Among the typical mitigating actions used in SIPS, generation rejection is widely applied to maintain transient stability in areas with excess of generation after a critical contingency. In fact, SIPS can readily and rapidly trip generators, under the assumption that the system can tolerate the subsequent generation-load imbalance [2]. This is the case of a critical SIPS of the BIPS, which is triggered by contingencies on the multi-infeed HVDC links connecting the main load center (in the southeast of Brazil) and the Belo Monte hydroelectric power plant (HPP) (in the north of Brazil). In terms of the dynamic performance of the BIPS, the most critical scenarios occur when the high voltage alternating current (HVAC) and HVDC interconnections operate highly loaded, and, as a consequence of strong AC-DC dynamic interactions, contingencies in the embedded HVDC links may affect the synchronism of the generators.

The development of Wide Area Monitoring Systems (WAMS) expanded the possibilities for the development of SIPS, allowing increased levels of observability and selectivity. The initiatives towards positioning additional Phasor Measurement Units (PMUs) at AC transmission substations, alongside the ongoing allocation of PMUs at the converter stations of the Belo Monte HVDC links, enable an enhanced monitoring of the embedded HVDC links and phase angle differences between the main geoeletric regions of the BIPS. Such possibilities constitute a promising scenario for the use of data-driven techniques with the aim of enhancing the arming process of the SIPS.

Several works have exploited WAMS and data-driven techniques in the design of SIPSs [3], but few of them target practical field implementations. In [1], [3], [4], applications of SIPSs around the world are provided, highlighting their respective types of mitigation actions, detection methods, and decision system architectures. In [5], a comprehensive guideline is presented for the design of SIPS, based on a survey of operational practices and industry knowledge. The work introduced in [6] proposes a SIPS to prevent blackouts in the Taiwan power system using PMU data. The proposed approach applies an instability prediction algorithm to avoid cascade tripping of relays. In [7], a SIPS is devised based on a set of PMUs strategically placed in the Argentine and Paraguayan power systems, aiming to support the operation of a new international interconnection. Hardware-in-the-loop (HIL) and field tests have shown that the designed SIPS is able to avoid loss of synchronism of relevant generating units in the interconnected system. In [8], a hierarchical deep learning machine model is proposed for the Guangdong power system, enabling quantitative and qualitative online transient stability predictions. In [9], a decision tree-based methodology is developed aiming to mitigate the risk of SIPS failure in the

Submitted to the 23rd Power Systems Computation Conference (PSCC 2024).

Norway power system. The approach involves sampling power system conditions to generate a large training data set for the decision tree model.

With respect to the state-of-the-art, the contributions of this work are the following: (a) design of a ML model allowing risk-averse decision making, mitigating occurrences of insufficient generation rejections to ensure transient stability; (b) design of a software application, developed in the openECA environment, encapsulating the ML model and data quality verification functions; (c) proof-of-concept tests and validation using a RTDS environment with control and protection replicas of the HVDC systems of the BIPS. Numerical results highlight that enhancements in selectivity may be achieved by using the customized ML model, fostering discussions of the benefits of applying synchrophasor data in the SIPSs of the BIPS.

This paper is organized as follows. Section II describes key aspects of the SIPS currently in operation with the aim of preserving the transient stability of the BIPS, as well as the developed framework of application. Section III presents the ML model designed to improve the current SIPS, along with the developed implementation using the openECA infrastructure. Section IV shows numerical results acquired through real-time HIL simulations conducted in collaboration with the Brazilian System Operator (BSO) towards a practical application of Wide Area Monitoring, Protection, and Control (WAMPACS) in the BIPS. Conclusions and final remarks are outlined in Section V.

## II. Developed Framework of Application

SIPSs are protection schemes designed to identify abnormal conditions and take predefined corrective actions [1], involving the use of local and remote measurements to characterize the operating conditions of a power system. With advances in computing, communication, and measurement technologies, sophisticated tools can be applied to improve the robustness and selectivity of conventional systemic protective actions. In particular, PMU data can enhance SIPSs by providing synchronized measurements of variables of interest, such as phase angle differences between phasor voltages at substations, which are closely tied to the dynamics of the main synchronous generators of bulk power systems.

In general, the SIPS deployment process can be divided into two phases: the planning and the operational phases, as defined by entities such as the IEEE [2] and ENTSO-E [10]. The planning phase covers the initial calculations to define the extent of the actions as well as the arming and triggering criteria. The operational phase comprises three essential execution steps, which can be summarized as follows: (a) *arming*: consists of determining the system state in which a contingency event might jeopardize the stable system operation; (b) *parameterization*: involves the adjustment of the SIPS parameters, taking into account information such as the availability of resources, mitigation costs, and potential contingencies that could lead to instability and subsequent blackouts; (c) *triggering*: this step encompasses the application of specific systems to monitor and detect critical contingencies

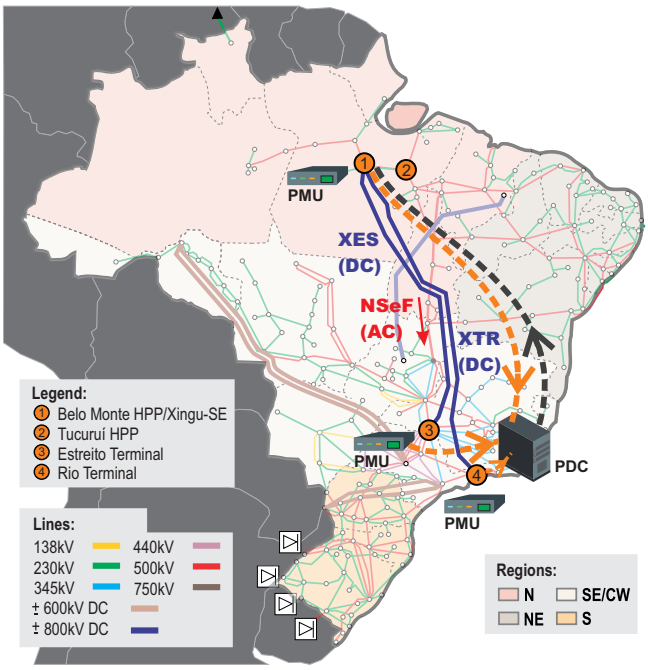


Fig. 1. Developed framework of application in the BIPS.

and to mitigate their effects, triggering predefined remedial actions in a timely manner. In Brazil, the fundamental design principles for SIPS have been outlined in [11]. This document, which is part of the Brazilian Grid Code, delineates the main steps to design, implement, and test a SIPS in the BIPS, establishing responsibilities to the BSO as well as to the generation, transmission, and distribution companies.

SIPS can be applied to avoid different phenomena in a power system, including transient stability problems arising from AC or DC transmission line contingencies. In the BIPS, which is composed of six HVDC bipoles in a multi-infeed configuration, forced outage on the HVDC links can severely deteriorate the rotor angle stability of the system, increasing the risks of large blackouts. Contingencies on one of the embedded HVDC links, either Xingu-Estreito (XES) or Xingu-Terminal Rio (XTR), both highlighted in Fig. 1, are the most critical contingencies in the current BIPS configuration. In the event of forced outages in these embedded HVDC links, a SIPS is triggered to reject generation at Belo Monte HPP within a maximum time period of 150 ms. The arming of the SIPS is sized using reference tables that relate the amount of rejected generation to the active power flow on the HVDC links and the active power flow on the North-South HVAC transmission lines.

This work focuses on applying PMU data and a risk-averse ML model to enhance the selectivity of the arming function of the SIPS associated with contingencies in the embedded HVDC links of the BIPS. In the proposed infrastructure, illustrated in Fig. 1, a Phasor Data Concentrator (PDC) acquires data from P Class compliant PMUs at converter stations, fostering the development of alternative solutions to improve the arming, parameterization, and triggering steps of the SIPS.

## III. Data-driven SIPS design and simulation

This section presents the proposed arming function developed to enhance the selectivity of the SIPS of the BIPS. Section III-A introduces the ML model designed to allow for risk-averse protective actions, taking into account PMU data. Section III-B describes the hardware and software infrastructure devised to test and validate the enhanced SIPS using HIL simulations.

### A. Designed ML model

The current SIPS has been parameterized using a series of simulation cases, assuming different amounts of generation rejection, with the aim of maintaining the stability of the system after forced outages in the embedded HVDC links. Tabular data can be retrieved from these simulation cases, gathering variables of interest to characterize prefault system conditions, such as active power flow through the North-South parallel HVAC transmission lines, as well as phase angle differences between the terminal buses in the Northern and Southern subsystems. Simulation results allow for the identification of the minimum amount of generation rejection required to guarantee the transient stability of the system for each case under analysis. The causal effect between a set of attributes that characterize the prefault system conditions and a set of possible number of units to be rejected can be featured as a multiclass classification problem, within the ML and statistical disciplines.

Multiclass classification problems can be addressed by data-driven techniques, such as artificial neural networks (ANN), decision trees, $k$-nearest neighbors, naive Bayes, support vector machines, and extreme learning machines. In this work, a multilayer feedforward ANN based model has been utilized, featuring a softmax activation function in its output layer, which is the algebraic simplification of results from $N$ logistic classifiers, normalized per class by the sum of the results of other $N-1$ logistic classifiers. The output then takes the form of a probability distribution, indicating the level of certainty at which a set of attributes modeling prefault system conditions finds a correspondence to a particular class of number of rejected generating units. Using a categorical cross-entropy loss function, quantifying the disparity between actual and predicted probabilities, model parameters/weights can be iteratively adjusted through supervised learning with the aim of bringing the output closer to the intended target. The categorical cross-entropy loss function can be expressed as

$$L^{\boldsymbol{\theta}} = -\frac{1}{N}\sum_{i=1}^{N} \alpha_i \log\left(p^{\boldsymbol{\theta}}_{C_{t_i}}(\mathbf{x}_i)\right) \tag{1}$$

where $\alpha_i$ is a balancing factor, weighting the loss function according to the number of samples in each class; $\mathbf{x}_i$ is the vector of input attributes for sample $i$; $\boldsymbol{\theta}$ denotes a vector of model parameters; $p^{\boldsymbol{\theta}}_{C_{t_i}}(\mathbf{x}_i)$ represents the predicted probability of the target class for sample $i$; and $N$ denotes the total number of samples in the data set.

The loss function in (1) is insensitive to predicted probabilities for non-target classes, since only the probabilities belonging to the target class are used as feedback in the training procedure. However, in real applications, achieving an accuracy of 100% is usually not feasible, and a certain probability of predicting non-target classes remains. This is appropriate in several scopes of application; however, in the context of maintaining transient stability, if an insufficient generation rejection is assigned, loss of synchronism is deemed to occur, affecting the security of supply. On the other hand, excessive generation rejection might lead to unwanted under-frequency load shedding, as a consequence of the load-generation imbalance. This implies the necessity to search for the elimination of the probability of insufficient generation rejection, favoring in turn a certain amount of over rejection to conservatively guarantee transient stability. This objective asymmetry can be modeled by sorting the classes in terms of the number of generation units to be rejected, as well as by splitting the contributions of the predicted target probability and the predicted above-class probabilities in the loss function as

$$L^{\boldsymbol{\zeta},\boldsymbol{\theta}} = -\frac{1}{N}\sum_{i=1}^{N} \alpha_i \left(L^{\boldsymbol{\zeta},\boldsymbol{\theta}}_{T_i}(\mathbf{x}_i) + L^{\boldsymbol{\zeta},\boldsymbol{\theta}}_{\mathcal{S}_i}(\mathbf{x}_i)\right) \tag{2}$$

where

$$\ell_{t_i} = \min(\ell, \left|\Omega_{C_{t_i}}\right|) \tag{3}$$

$$L^{\boldsymbol{\zeta},\boldsymbol{\theta}}_{T_i}(\mathbf{x}_i) = \left(1 - \sum_{k=1}^{\ell_{t_i}} \zeta^{C_{t_i}}_{C_{t_i+k}}\right) \log\left(p^{\boldsymbol{\theta}}_{C_{t_i}}(\mathbf{x}_i)\right) \tag{4}$$

$$L^{\boldsymbol{\zeta},\boldsymbol{\theta}}_{\mathcal{S}_i}(\mathbf{x}_i) = \sum_{k=1}^{\ell_{t_i}} \zeta^{C_{t_i}}_{C_{t_i+k}} \log\left(p^{\boldsymbol{\theta}}_{C_{t_i+k}}(\mathbf{x}_i)\right) \tag{5}$$

in which $\Omega_{C_{t_i}}$ denotes the set of classes above the target class for the sample $i$; $\ell$ is a threshold number of classes above the target class to be considered in the analysis; $L^{\boldsymbol{\zeta},\boldsymbol{\theta}}_{T_i}(\mathbf{x}_i)$ and $L^{\boldsymbol{\zeta},\boldsymbol{\theta}}_{\mathcal{S}_i}(\mathbf{x}_i)$ are the contributions of the predicted target probability and the predicted probabilities of the above classes, respectively, for the sample $i$. For a given class $C_r$, $\zeta^{C_r}_{C_{r+k}}$ are the components of a target probability mass function expressed as

$$p^{\boldsymbol{\zeta}}_{C_r} = \left[1 - \sum_{k=1}^{\ell_r} \zeta^{C_r}_{C_{r+k}}, \zeta^{C_r}_{C_{r+1}}, \ldots, \zeta^{C_r}_{C_{r+\ell_r}}\right]^T \tag{6}$$

The decision parameter vector $\boldsymbol{\zeta}$ is a vector with entries $\zeta^{C_r}_{C_{r+k}}$, $\forall r = 1, \ldots, N_c$, where $N_c$ denotes the number of classes. Decision makers can use different patterns of target probability mass functions $p^{\boldsymbol{\zeta}}_{C_r}$ to customize a risk-averse perspective for each class under analysis.

The designed ANN has been conceived with two intermediate layers using the Exponential Linear Unit as activation function. The Adam optimization algorithm [12] has been used to iteratively adjust model weights during training, by minimizing (2) using an improved stochastic gradient descent method, which incorporates an adaptive estimation of first- and second-order moments. A metric has been developed to

monitor and measure the performance of the model during training and testing. It evaluates the average probability of insufficient rejection as

$$M^{\boldsymbol{\zeta},\boldsymbol{\theta}} = \frac{1}{N}\sum_{k=1}^{\varrho_{t_i}} p^{\boldsymbol{\theta}}_{C_{t_i-k}}(\mathbf{x}_i) \tag{7}$$

where $\varrho_{t_i}$ stands for the number of classes below class $C_{t_i}$, corresponding to classes corresponding with insufficient generation rejection.

In case an optimized set of target probability mass functions is required, aiming to support the customization of a risk-averse solution, a hyperparameter optimization problem can be formulated as

$$\min f(\boldsymbol{\zeta}) = \sum_{r=1}^{N_c}\left(\sum_{k=1}^{\ell_r} b_k \zeta^{C_r}_{C_{r+k}}\right) \tag{8}$$

s.t.

$$\sum_{k=1}^{\ell_r} \zeta^{C_r}_{C_{r+k}} \leq 1, \forall r = 1,\ldots,N_c \tag{9}$$

$$M^{\boldsymbol{\zeta},\boldsymbol{\theta}} \leq p_{lim} \tag{10}$$

where $b_r$ is a non-negative real value such that $b_r >> b_{r+1}$, $\forall r = 1,\ldots,N_c - 1$, and $p_{lim}$ is an acceptable average probability of insufficient rejection. In the proposed application framework, the BSO has dictated that $p_{lim}$ must be adjusted aiming at the null risk of transient instability, considering the set of samples under analysis.

### *B. Designed real-time simulation environment*

Although conventional dynamic simulations provide a relatively rapid way of generating data for ML training, real-time simulation tests are of utmost importance to validate proposed approaches intended for practical use in the field. A real-time simulation environment has been designed to support testing and validating the enhanced SIPS. Hardware-in-the-loop and software infrastructure are described in Section III-B1 and III-B2, respectively.

*1) Hardware-in-the-loop infrastructure:* The proposed approach has been validated using a RTDS, capable of simulating electromagnetic transient phenomena in real time. The BIPS is modeled in RSCAD, a software package built within the RTDS, using an equivalent representation provided with dynamic models of relevant components, aiming to simulate the main electromechanical oscillations among synchronous machines in the North and Southeast subsystems. By utilizing the RSCAD/RTDS infrastruture, the conditions of the BIPS during contingencies on the embedded HVDC bipoles can be simulated, enabling the testing of the remedial actions required to stabilize the power system. The resulting infrastructure takes advantage of the capabilities of the RSCAD/RTDS infrastruture, by representing the control and protection cubicles of the XES and XTR bipoles with replicas provided by the transmission companies.

With the aim of enabling the PMU function within the RSCAD/RTDS infrastructure, two distinct hardware elements have been installed: the GTSYNC synchronization card and the GTNETx2 Giga-Transceiver network communication card. The GTSYNC synchronization card is used to synchronize the simulation time with an external GE RT430 GNSS clock, referenced to the GPS and GLONASS satellites. The GTNETx2 Giga-Transceiver network communication card facilitates real-time interaction with the simulator, enabling Ethernet connectivity. The GTNET-PMU firmware allows the network communication card to provide synchrophasor output data streams in compliance with the IEC/IEEE 60255-118-1 standard. The GTNET-PMU firmware can be configured to provide symmetric component or individual phase data related to three-phase voltages and currents, using UDP or TCP connections. The frame rate of each PMU is set to 60 frames per second.

In order to collect the generated data and perform real-time application testing, a PDC is built on a Dell PowerEdge R640 Server. The server is equipped with 2 Intel Xeon Gold 5222 processors, 64 GB of RAM, 2x 1 Gbps network cards, with data storage capacity of 2 TB. This setup is referred as RSCAD/RTDS/PMU/PDC infrastructure.

*2) Software infrastructure:* Within the PDC server, Grid Protection Alliance (GPA) open-source software components known as Open Phasor Data Concentrator (openPDC) and openECA are applied. The openECA serves as a platform designed to facilitate the creation of processes and analyses that involve the use of synchrophasors. This software provides the necessary framework for constructing application prototypes aimed at real-time decision making, offering the capability to effectively process synchrophasor measurements acquired through the configured GTNET-PMU boards.

The openECA software is utilized to specify the input and output data structures and to manage the mapping of structures with their corresponding sources on the GTNET-PMU boards. The openECA software is used to produce an External Application (EA) with open source code in C# language, serving as an environment to code embedded functions to, for instance, verify data quality and execute ML models. The ML model becomes an integral part of the EA by using the Open Neural Network Exchange (ONNX) library [13], which allows the integration of pre-trained ANN models using a standardized file format (.onnx), making it possible to deploy these models across various platforms and programming languages. Essentially, the ONNX library assumes the pivotal role of uploading and executing the ML model within the real-time simulation framework.

The diagram in Fig. 2 shows the main components that comprise the real-time simulation environment and highlights the associated communication protocols. The real-time process begins with the activation of the RTDS, which contains the necessary parameters to simulate the dynamic equivalent system of the BIPS under the conditions of interest. The GTNET-PMU boards provide the desired measurements, which are conveyed using the IEEE C37.118-2 protocol [14] to the PDC Server, where the openPDC and openECA softwares are executed.

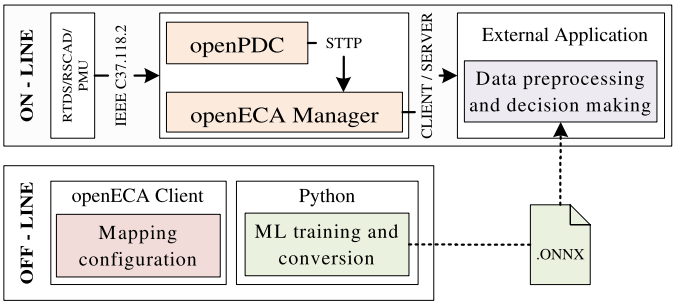


Fig. 2. Designed real-time simulation environment.

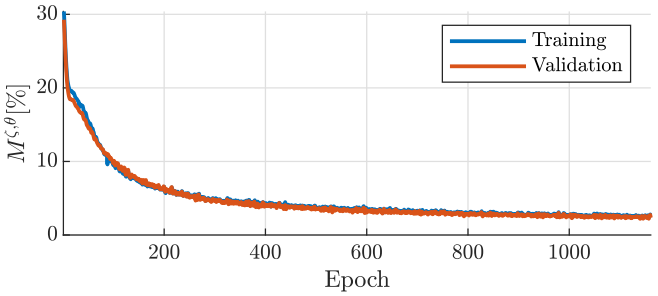


Fig. 3. Convergence of the performance metric.

During an off-line development stage, the ANN is trained using an application coded in the Python programming language, with support of widely recognized packages such as the TensorFlow [15]. Within the EA, the computations related to retrieving the ML attributes are carried out using measurements provided by the GTNET-PMU boards, which are requested from the EA in real time according to the mapped input structures. The attributes are then processed by the ML model, which outputs the necessary amount of generation units to be rejected, with the aim of maintaining the angular stability of the system.

The EA is called every time an additional measurement is received, even if, at the moment of reception, other measurements with the same timestamp are not available. Data quality verification functions are executed to interpret quality-related fields in transmitted frames [14], as well as to handle the composition of blocks of attributes. From the moment that a block of attributes with the same timestamp is complete, the block is sent to a thread that executes the ML model. To handle redundancies in variables of interest, data with better-recognized accuracy are prioritized in the composition of each block. In case one of the required attributes is unavailable, or a non-temporary loss of frame is identified, the enhanced arming is disabled and the conventional arming, associated to the current SIPS, must be applied. The enhanced arming is also disabled in the absence of steady-state operation, since the ML model is trained with steady-state prefault conditions. Through signals indicating steady-state operation and required data availability, an enabling signal is formed, which is sent to a master application along with the number of generating units to be rejected in case of forced outage in the embedded HVDC links.

## IV. Numerical Results

The EA has been configured to receive the following attributes, acquired with electromechanical simulations: angular difference between the HVDC converter stations (`AngDif`), the active power flow through the North-South parallel HVAC interconnection (`NSeF`), total power generated at two important generating centers in the North region and the power produced in generation clusters in the Southeast region. The operating conditions under consideration primarily involve cases with heavily loaded HVDC/HVAC interconnections, where the attributes fall within the following ranges: 16.4 to 72.9 electrical degrees for AngDif; 0 to 2.4 GW for NSeF; 8.3 to 11 GW and 5.5 to 8.5 GW for two hydroelectric power plants (HPP) in the North region; and 10.3 to 13.2 GW for the generation clusters in the Southeast region. The number of rejected generating units to be selected by the arming function ranges from 2 to 7 units, representing six classes for the ML model. The threshold number of classes $\ell$ and the probability $p_{lim}$ are specified as 1 and 2.8%, respectively.

TABLE I
Comparative results between the proposed model and a reference model

| | Proposed model | Reference model |
|---|---|---|
| Accurate rejection | 96,43% | 94,64% |
| Above-class rejection | 3,57% | 3,57% |
| Below-class rejection | 0% | 1,79% |

For an optimized $\zeta$ of 0.185, the proposed model has produced results with 0% of insufficient generation rejections with smooth convergence of the performance metric, as shown in Fig. 3. Results for the proposed model are compared in Table I with those obtained with a reference model, which has been trained using the reference loss function in (1). Using the reference loss function, 94.64% of the samples have been correctly assigned with the minimum number of generating units required to achieve angular stability, in the case of forced outage in the embedded HVDC bipoles. Approximately 3,57% of the results correspond to above-class rejections, all of which refer to only one generating unit above necessary. However, insufficient generation rejections can be retrieved with the reference model, amounting 1,79% of the outcomes, thereby offering risks to the security of the BIPS operation. By applying the proposed model, the results related to accurate rejections have increased to 96.43%. Insufficient generation rejections are eliminated, while the proportion of above-class rejections of 3,57% remains unchanged.

Using the ML model, real-time simulations have been performed with the aim of illustrating key aspects of the developed application.

### A. Loss of PMU data

In this experiment, the loss of PMU signals used to compute the attribute `AngDif` and `NSeF` is simulated sequentially.

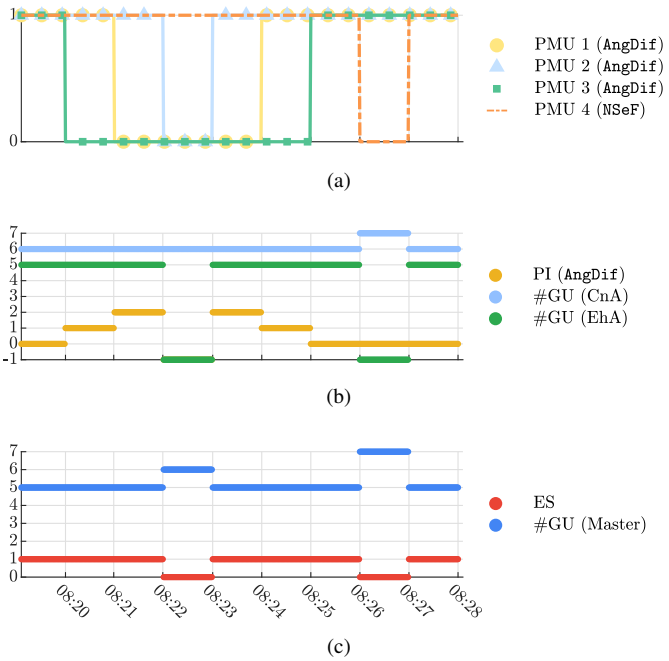


Fig. 4. SIPS arming in case of loss of PMU data.

After the unavailability of the sources, the lost signals are also reactivated sequentially. This simulation has been performed to test the redundancy management and unavailability detection functions. The results are shown in Fig. 4. In Figure 4a, a logic signal pointing to the availability of the attribute `AngDif`, in accordance with the availability of PMUs, is shown. PMU 1, 2 and 3 are necessary for the computation of the attribute `AngDif`, while data from PMU 4 are used to compute the attribute `NSeF`, which has been simulated without redundancy. Initially, all PMUs are active, assuming the Boolean value 1. At 08:20, PMU 1 (green) becomes inactive, followed by PMU 2 (yellow) and PMU 3 (blue) at 08:21 and 08:23, respectively. PMU 3 is reactivated at 08:23, followed by PMU 2 and PMU 1, at 08:24 and 08:25, respectively. At 08:26, PMU 4 is deactivated and, after one minute, reactivated.

In Fig. 4b, the effects of PMU deactivation on the conventional and enhanced arming can be observed. A priority indicator (PI), shown in dark yellow for the attribute `AngDif`, assumes the value 0, 1 and 2 (arranged from highest to lowest priority), corresponding to the disconnection of PMU 1, 2 and 3. When PMU 1 is disconnected, the PI assumes the value 1 and when PMU 2 is disconnected, the PI assumes the value 2. Between 08:22 and 08:23, PMUs 1, 2 and 3 are all disconnected, causing the attribute `AngDif` to be unavailable. During this period, PI assumes the value -1. As PMUs 3, 2 and 1 are reactivated, the PI assumes values 2, 1 and 0. Fig. 4b also shows the number of generating units to be rejected according to the assumed conventional arming (CnA), in blue, and the enhanced arming (EhA), in green. The conventional arming assigns the rejection of 6 to 7 generating units, depending upon the availability of the attribute `NSeF`, which is sourced from PMU 4. The number of generating units to be rejected by the enhanced arming is 5, a value retrieved by executing the ML model, assuming that the attributes `AngDif` and `NSeF` are available.

In case `AngDif` or `NSeF` are unavailable, the enhanced arming is disabled. This is shown in Fig. 4c, where the enabling signal (ES), in red, goes from 1 to 0, between 08:22 and 08:23, as well as 08:26 and 08:27. In Fig. 4c the arming selected by the master application is presented as a combination of conventional and enhanced arming. The master application gives priority to the enhanced arming, that is, the conventional arming is used only when the enhanced arming is disabled. The master application sends the arming decision to a dedicated protection system at the Belo Monte HPP, responsible for reacting to a HVDC link emergency switch off signal, produced at the Xingu converter station.

### *B. Rejection of generating unit*

In this experiment, variations in the angular differences between areas are simulated through the disconnection of one generating unit in the Belo Monte HPP. The purpose of this simulation is to observe the performance of the routine devoted to detect the loss of steady-state condition. In Fig. 5a, its possible to observe the effect of rejecting the generating unit, causing oscillations in the attribute `AngDif`. The angular difference has a transient variation ranging from 55° to approximately 35°, stabilizing roughly at 44°.

In Fig. 5b, it is observed that the transient effects caused by generation rejection have been correctly identified. Before 01:26:23, the attribute `AngDif` is approximately 55°, and the enhanced arming indicates 5 generating units, following the ML model. At 01:26:23, the steady-state indicator (SSI), in red, assumes the value 0, indicating the absence of steady-state condition, and remains in this condition until 01:26:35, when the rate of change of the attribute `AngDif` assumes values lower than a specified threshold. Due to the identification of transient operation conditions, enhanced arming is disabled. Between 01:26:23 and 01:26:35, the conventional arming is selected by the master application, indicating 6 generation units to be rejected. At 01:26:35, when the SSI returns to value 1, the enhanced arming is enabled and indicates 4 generating units due to the change in operation conditions caused by the event.

### *C. Forced outage of the HVDC bipole*

This experiment consists of a contingency on the embedded HVDC bipole XES, representing an outage of 4,000 MW, without power transfer to the remaining bipole XTR, followed by the rejection of 6 generation units in Belo Monte (HPP), 150 ms after the event. The simulated event can be seen in Fig. 6a, which shows the HVDC power flow (dark yellow) changing from 4000 MW to 0 MW at the instant of the forced outage in the XES bipole. Fig. 6b shows the effect on the attribute `AngDif`, which goes from a steady-state condition, at approximately 53°, to a transient condition, with a maximum swing angle of 110°. At 08:23:27, the tripping signal (TS), in orange, immediately assumes value 1, as shown in Fig. 6c.

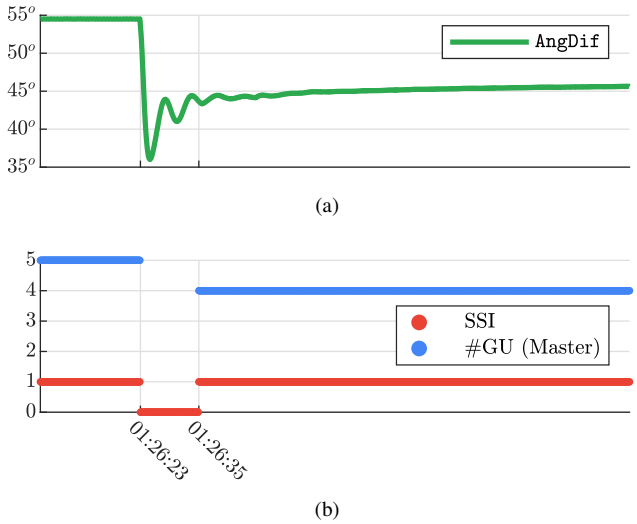


Fig. 5. SIPS arming in case of loss of steady-state condition.

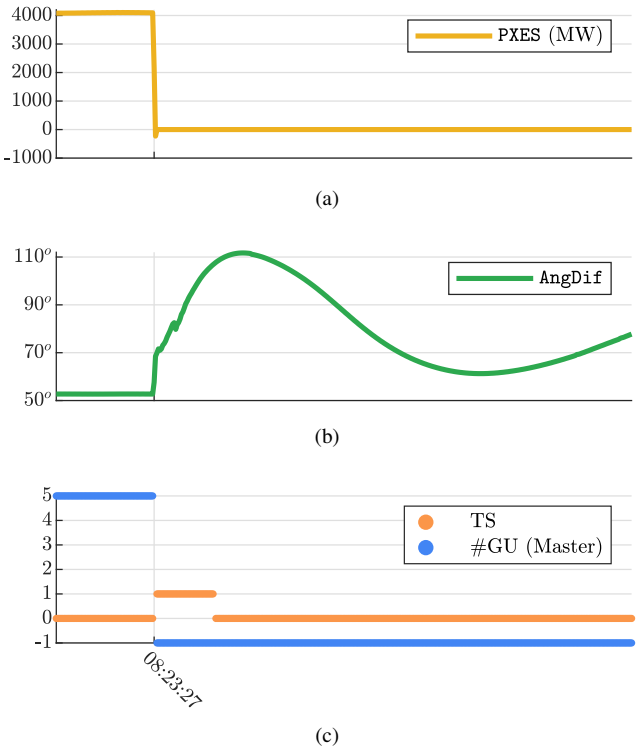


Fig. 6. SIPS triggering due to forced outage of the HVDC bipole.

This tripping signal serves as backup for a primary tripping signal sent to a dedicated system at Belo Monte HPP, after the occurrence of an emergency switch off at the embedded HVDC link.

## V. Conclusions and Final Remarks

The modeling and implementation of a customized ML model is the focus of this work, where synchrophasor data is used to enhance the arming procedure of a critical SIPS of the BIPS. Risk-averse decision-making, mitigating loss of selectivity conditions, is achieved by modeling an alternative loss function with the aim of avoiding insufficient generation rejections. Implementation has been described, highlighting the specification of an RSCAD/RTDS/PMU/PDC infrastructure, the usage of the openECA software environment, the application of data quality verification functions, and the embedding of the ML model within the software framework. Numerical results emphasize the effectiveness of the ML model in mitigating cases of insufficient generation rejections, in order to guarantee the transient stability of the BIPS, in cases of forced outage of the HVDC links. The results using HIL simulations show the appropriate functioning of the approach in cases of loss of PMU data, loss of steady-state conditions, and forced outage of the HVDC links.

Future works are envisioned to carry out a pilot project with field implementations at the corresponding HVDC converter stations in Brazil. The impact of communication latency on the robustness of the application is an aspect to be analyzed in the pilot project. Moreover, the ML model is expected to be expanded, taking into account the PMU data currently available in the Brazilian WAMS, as well as data associated to post-fault conditions.

## Acknowledgement

This work has been supported by the State Grid Brazil Holding S.A. (project code PD-10307-0221/2022), within the scope of the ANEEL R&D Programme. The work has been also supported by Brazilian Independent System Operator (project code OC_0001856).

## References

[1] S. Stanković, E. Hillberg, and S. Ackeby, "System integrity protection schemes: Naming conventions and the need for standardization," *Energies*, vol. 15, no. 11, p. 3920, 2022.

[2] IEEE, "IEEE guide for engineering, implementation, and management of system integrity protection schemes," *IEEE Std C37.250-2020*, pp. 1–71, 2020.

[3] N. K. Rajalwal and D. Ghosh, "Recent trends in integrity protection of power system: A literature review," *International Transactions on Electrical Energy Systems*, vol. 30, no. 10, p. e12523, 2020.

[4] M. Arabzadeh, H. Seifi, and M. K. Sheikh-El-Eslami, "A new mechanism for remedial action schemes design in a multi-area power system considering competitive participation of multiple electricity market players," *International Journal of Electrical Power & Energy Systems*, vol. 103, pp. 31–42, 2018.

[5] V. Madani, D. Novosel, S. Horowitz, M. Adamiak, J. Amantegui, D. Karlsson, S. Imai, and A. Apostolov, "IEEE PSRC report on global industry experiences with system integrity protection schemes (SIPS)," *IEEE Transactions on Power Delivery*, vol. 25, no. 4, pp. 2143–2155, 2010.

[6] Y. J. Wang, C. W. Liu, and Y. H. Liu, "A PMU based special protection scheme: a case study of taiwan power system," *International Journal of Electrical Power & Energy Systems*, vol. 27, no. 3, pp. 215–223, 2005.

[7] J. M. B. Godoy, R. A. de Oliveira, G. Aguayo, E. Rodriguez, A. J. M. Szostak, J. A. dos Santos, A. P. Tochetto, M. L. S. Rios, P. H. Galassi, J. R. Pesente *et al.*, "The eccande project: Design, field implementation, and operation of a special protection scheme based on synchronized phasor measurements," *IEEE Transactions on Power Delivery*, 2022.

[8] L. Zhu, D. J. Hill, and C. Lu, "Hierarchical deep learning machine for power system online transient stability prediction," *IEEE Transactions on Power Systems*, vol. 35, no. 3, pp. 2399–2411, 2020.

[9] V. Krishnan and J. D. McCalley, "Role of statistical and machine learning methods in special protection scheme logic design and failure assessment," *Electric Power Components and Systems*, vol. 44, no. 11, pp. 1215–1224, 2016.

[10] ENTSO-E, "Special protection schemes," ENTSO-E, Brussels Belgium, Tech. Rep., 03 2012.
[11] ONS, "Special Protection Systems - Module 11 - Submodule 11.4," ONS, Tech. Rep., 2007 (in portuguese).
[12] D. Kingma and J. Ba, "Adam: A method for stochastic optimization," *International Conference on Learning Representations*, 12 2014.
[13] J. Bai, F. Lu, K. Zhang *et al.*, "Onnx: Open neural network exchange," https://github.com/onnx/onnx, 2019.
[14] IEEE, "IEEE standard for synchrophasor data transfer for power systems," *IEEE Std C37.118.2-2011 (Revision of IEEE Std C37.118-2005)*, pp. 1–53, 2011.
[15] M. Abadi, A. Agarwal, P. Barham, E. Brevdo, Z. Chen, C. Citro, G. S. Corrado, A. Davis, J. Dean, M. Devin *et al.*, "TensorFlow: Large-scale machine learning on heterogeneous systems," 2015, software available from tensorflow.org. [Online]. Available: https://www.tensorflow.org/